PressureCap

Mitrakos, Vasileios; Cummins, Gerard; Tauber, Faulk J.; Cox, Benjamin F.; Pavaluri, Sumanth K. ; Wood, Graham S.; Potter, Mark A.; Clutton, Eddie ; Cochran, Sandy; Speck, Thomas ; Hands, Philip J.W.; Desmulliez, Marc P.Y.

DOI:
10.1016/j.device.2024.100325

Device

Article

PressureCap: An endoscopic sensor capsule for real-time gastrointestinal pressure monitoring

Graphical abstract

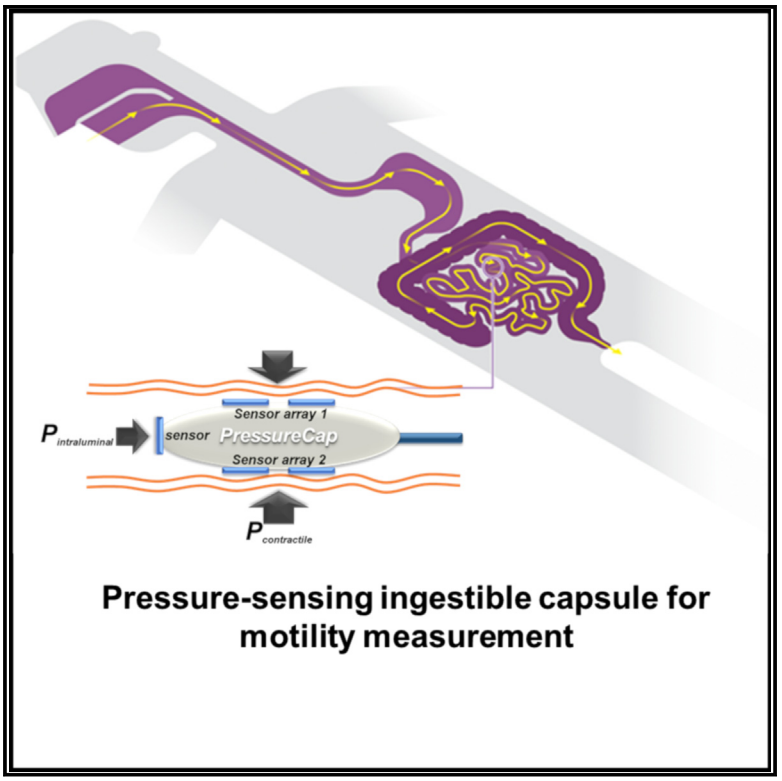

Authors

Vasileios Mitrakos, Gerard Cummins, Falk J. Tauber, ..., Thomas Speck, Philip J.W. Hands, Marc P.Y. Desmulliez

Correspondence

g.cummins@bham.ac.uk (G.C.), m.desmulliez@hw.ac.uk (M.P.Y.D.)

In brief

An ingestible pressure-sensing pill that can capture information on gastrointestinal motility through the use of an array of microfabricated, flexible, wireless LC pressure sensors integrated onto the pill surface has been developed. The pill has been tested using *in vitro* and *in vivo* models and has been shown to detect changes in motility.

Highlights

- Development of an ingestible pill for monitoring gastrointestinal motility
- The pill can measure contractile and intraluminal pressure
- Measurement is done with an array of wireless pressure sensors fixed on the pill
- The pill has captured motility events *in vivo*

Validate
Functional device with real-world testing, ready to scale

Mitrakos et al., 2024, Device *2*, 100325
June 21, 2024
https://doi.org/10.1016/j.device.2024.100325

CellPress

Please cite this article in press as: Mitrakos et al., PressureCap: An endoscopic sensor capsule for real-time gastrointestinal pressure monitoring, Device (2024), https://doi.org/10.1016/j.device.2024.100325

Device

CellPress
OPEN ACCESS

Article

PressureCap: An endoscopic sensor capsule for real-time gastrointestinal pressure monitoring

Vasileios Mitrakos,[1,2,3] Gerard Cummins,[1,4,5,*] Falk J. Tauber,[6] Benjamin F. Cox,[7,8] Sumanth K. Pavuluri,[1] Graham S. Wood,[3] Mark A. Potter,[9] Eddie Clutton,[10] Sandy Cochran,[11] Thomas Speck,[6] Philip J.W. Hands,[3] and Marc P.Y. Desmulliez[1,12,*]

[1]Smart Systems Group, Institute of Sensors, Signals, and Systems, School of Engineering and Physical Sciences, Heriot-Watt University, Edinburgh EH14 4AS, UK
[2]Touchlab, National Robotarium, Heriot-Watt University, Edinburgh Campus, Edinburgh EH14 4AS, UK
[3]Institute for Integrated Micro & Nano Systems (IMNS), School of Engineering, University of Edinburgh, Edinburgh EH9 3FB, UK
[4]School of Engineering, University of Birmingham, Edgbaston B15 2TT, UK
[5]Healthcare Technologies Institute, University of Birmingham, Edgbaston B15 2TT, UK
[6]Plant Biomechanics Group and Botanic Garden, University of Freiburg, Freiburg, Germany
[7]University of Dundee, Dundee DD1 4HN, UK
[8]Saba University School of Medicine, The Bottom, Saba, Caribbean, the Netherlands
[9]Department of Colorectal Surgery, Western General Hospital, Edinburgh EH4 2XU, UK
[10]The Royal (Dick) School of Veterinary Studies and Roslin Institute, University of Edinburgh, Easter Bush, Roslin, Midlothian EH25 9RG, UK
[11]James Watt School of Engineering, University of Glasgow, Glasgow G12 8QQ, UK
[12]Lead contact
*Correspondence: g.cummins@bham.ac.uk (G.C.), m.desmulliez@hw.ac.uk (M.P.Y.D.)
https://doi.org/10.1016/j.device.2024.100325

THE BIGGER PICTURE Gastrointestinal (GI) motility refers to the movement of the digestive system and the transit of its contents, such as food and waste. This movement is crucial for digesting food, absorbing nutrients, and expelling waste. Many dysfunctions of the GI tract are often associated with atypical motility. These are usually clinically diagnosed by measuring the change in pressure within the GI tract by manometry, which involves inserting a pressure-sensing tube into the body. Various pressure-sensing ingestible capsules have recently been developed, but often use a limited number of sensors, which constrains the quality of information gathered on motility. In this work, we report on the development and characterization of an ingestible device that contains an array of wireless, flexible pressure sensors on the surface of the capsule that can capture greater detail about motility.

SUMMARY

Functional gastrointestinal (GI) disease associated with abnormal GI motility has an adverse impact on the quality of life of those affected. High-resolution manometry has improved the diagnosis of these conditions, enabling motility measurement, but these tools are limited in that they cannot access the entire length of the GI tract. Other solutions, such as the SmartPill ingestible motility capsule, only measure the transit times between the regions of the GI tract and provide information on the luminal component of GI pressure. Measuring both luminal and contractile pressure caused by peristalsis would improve the diagnosis of abnormal motility. Here, we report an ingestible capsule encapsulated with a flexible pressure sensor array. The capsule can detect changes in both contractile and luminal GI pressure in an *in vitro* peristaltic tissue phantom and in porcine animal models. These findings promise high-resolution, sensitive, multisite pressure measurements currently not possible with other ingestible motility capsules.

INTRODUCTION

With a prevalence in the general population reported to be between 5% and 15%,[1] functional gastrointestinal diseases (FGIDs) disrupt normal GI function and significantly affect the quality of life of those affected.[2] An estimated 40% of FGIDs are associated with abnormal GI motility (dysmotility),[3,4] which refers to the movement of the GI tissue and the transit of the contents within it. The introduction of high-resolution manometry has improved the diagnosis of FGID, allowing objective measurement of GI motility. Conventional endoscopic high-resolution manometry procedure relies on the use of a catheter

Please cite this article in press as: Mitrakos et al., PressureCap: An endoscopic sensor capsule for real-time gastrointestinal pressure monitoring, Device (2024), https://doi.org/10.1016/j.device.2024.100325

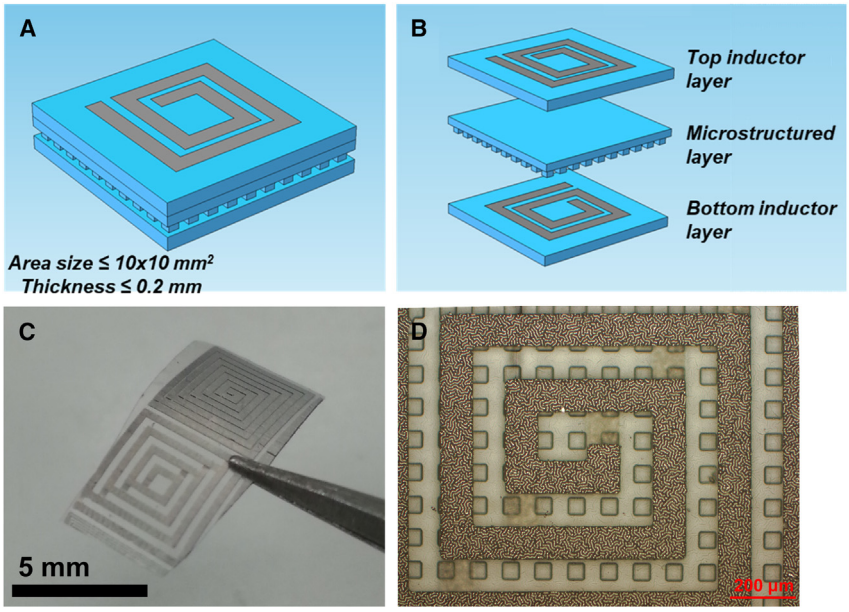

Figure 1. Schematic diagrams and photographs of the flexible LC sensors' design and structure

(A) Isometric schematic image of the flexible pressure sensor.

(B) Magnified view of sensor, showing top inductor layer, microstructured intermediate layer with frustra, and bottom inductor layer.

(C) Image of fabricated flexible pressure sensor.

(D) Magnified view showing wrinkled metallic thin film inductor tracks.

populated by a series of solid-state pressure sensors protruding from its surface, inserted inside a patient via his/her nose and steered manually toward the small intestine through the stomach. The array of pressure sensors captures the contractile behavior of the GI tract, typically the esophagus or colon, which the physician then assesses to help diagnose the dysmotility afflicting the patient. These devices are unable to access the full length of the small intestine because inserting and navigating the catheter within the far depths of the small intestine proves to be extremely difficult due to its excessive length and highly convoluted shape. This tool must, however, be steered by a trained physician[5]; it also causes patient discomfort[5] and cannot access the entire length of the GI tract.[6]

Recent advances in the field of ingestible sensing[7,8] have led to the development of ingestible motility capsules (IMCs) capable of measuring pressure continuously and in real time along the entire GI tract with minimal discomfort to the patient.[9] Another advantage of acquiring the pressure profile via an IMC is the potential for replacing conventional antroduodenal and colonic studies with a method that has much higher patient tolerance. Such medical procedures are typically used to distinguish visceral neuropathy from myopathy, which may be another potential cause of the observed dysmotility of a patient.[10] The SmartPill is the only US Food and Drug Administration-approved capsule with pressure-sensing capability currently on the market.[11] The single pressure sensor has an operating range of 0–46 kPa and a sensitivity of ±0.650 kPa. Aided by integrated pH and temperature sensors, this endoscopic capsule measures transit times between the separate regions of the GI tract.

Pressure within the GI tract results from the intraluminal pressure caused by changes in abdominal pressure and the contractile pressure stemming from the contraction of intestinal musculature due to peristalsis.[12] Capturing the entire pressure profile by an IMC would provide additional motility information to that obtained from measuring the transit times. A single pressure sensor, as found in the SmartPill and other pressure-sensing capsules reported in the literature,[5,6,13] only measures intraluminal pressure. To the best of the authors' knowledge, only two capsules have incorporated two orthogonally oriented pressure sensors for detecting both intraluminal and contractile pressures.[14,15] From a clinical perspective, the use of only two sensors is inefficient in differentiating visceral neuropathy from myopathy[10]; our design incorporates five sensors. Many commercially available rigid pressure sensors also use a large portion of the available capsule volume, limiting the integration of additional pressure sensors, let alone other sensing modalities. In addition, the reliance on silicone oil in such designs makes them susceptible to sensor drift due to oil leakage[16] or requires extensive adjustment of the volume of oil before use to obtain the desired internal pressure for the transducer.[15] The new design allows the classification of patients suffering from gastroparesis into severity and subtype categories, expressed by the significant decrease in stomach contractions[17] or the variations in contractile patterns within the large intestine that have been associated with different types of chronic constipation.[18] Acquiring these patterns could also offer a more in-depth understanding of the pathophysiologic mechanisms that govern the emergence of these variations.[6]

In this article, a wireless flexible thin film inductive-capacitive (LC) pressure sensor is applied to the outer surface of a tethered capsule to create a novel IMC capable of continuous monitoring of GI motility. The pressure sensor uses a bottom-up microfabrication process to achieve the desired sensitivity, tunability, and conformability required for this application. Flexible pressure sensors are playing an increasingly important role in next-generation healthcare devices and are capable of sensing cutaneous touch, monitoring blood flow, advancing biomimetic prostheses, repairing tendons, and tracking the progression of intraocular glaucoma, to name but a few applications.[19] These flexible pressure sensors can operate using piezoresistive,[20] piezoelectric,[21] triboelectric,[22] or capacitive principles,[23] but those based on LC principles have the advantage of a highly linear response to pressure and a fully passive wireless operation via near-field inductive coupling with a coil antenna (inductor) without the need of any interconnections to the readout or direct power supply.

The fully passive nature of LC sensors has already been validated in healthcare applications that demand a highly sensitive

Please cite this article in press as: Mitrakos et al., PressureCap: An endoscopic sensor capsule for real-time gastrointestinal pressure monitoring, Device (2024), https://doi.org/10.1016/j.device.2024.100325

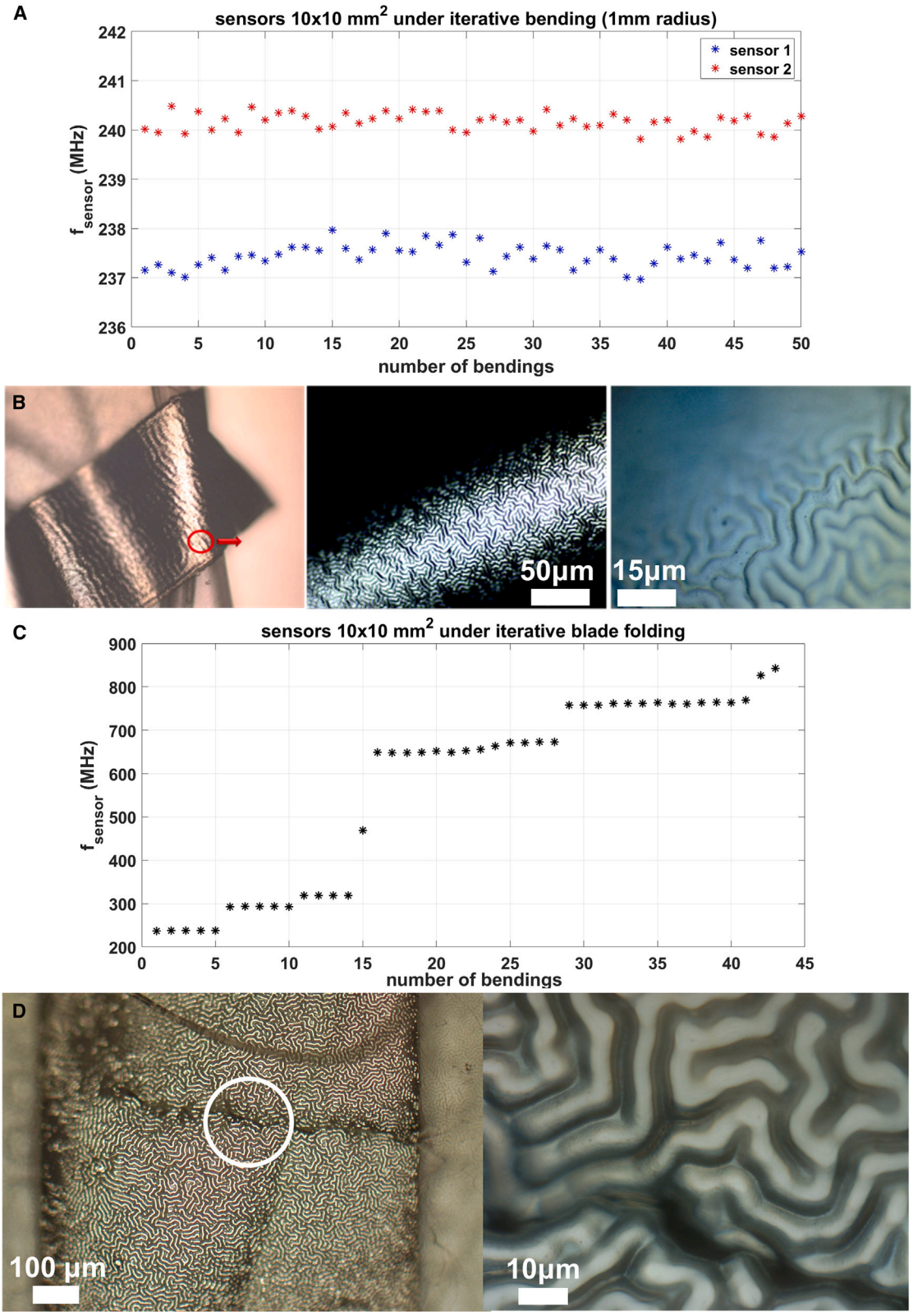

(legend on next page)

Please cite this article in press as: Mitrakos et al., PressureCap: An endoscopic sensor capsule for real-time gastrointestinal pressure monitoring, Device (2024), https://doi.org/10.1016/j.device.2024.100325

response and a minimally invasive sensing module that does not required wiring. Examples include intraocular pressure monitoring,[24,25] chronic implantation for bone or wound healing monitoring,[26] intracranial pressure monitoring,[27] and arterial blood flow monitoring.[28] Within the context of capsule manometry, wired sensors instead require strict capsule hermiticity requirements due to the need of vias or holes in the capsule shell that can adversely affect the enclosed electronics and limit the available space. Flexible LC sensors can achieve low detection limits, high and tunable sensitivity, and millisecond response and relaxation times (no hysteresis), as well as a highly stable performance to compressive cycling.[19] Of equal significance within the context of flexible sensors is the conformability of the sensor structure to high radii bending without failure. Currently, the majority of the reported LC sensors use relatively rigid materials such as polyimide as the substrate for the electrode layers of the sensor over soft elastomers such as polydimethylsiloxane (PDMS), which limits the conformability of the sensors to relatively large bending radii of 27 mm[27] that exceeds the bending radii limits of an ingestible capsule. The flexible pressure sensor array proposed in this study can be integrated into the outer surface of the shell due to its conformability, enabling multiple measurements of the GI contractile pressure in the range of 0–25 kPa acting on the IMC with a resolution of 0.2 kPa necessary to capture weak peristaltic contractions.

RESULTS

Sensor characterization

The flexible LC pressure sensors consist of two wrinkled thin film metal inductors on PDMS sheets separated by a microstructured PDMS layer forming an array of frustra for increased sensitivity, as shown in Figure 1. The two-dimensional spatial patterning of the microfrustra was specifically chosen with two design criteria in mind. First, the fill factor was chosen to reduce the average Young's modulus and provide the desired compressibility (and hence sensitivity) of the capacitive sensing layer. Second, the specific size and spacing of the microfrustra were chosen such that frustra were small enough to provide uniform deformation over the sensor area, while also being large enough to maintain good adhesion with the adjoining layers and hence avoid delamination under shear forces. The analytical model and microfabrication process detailing this sensor can be found in Notes S1 and S2, and in the associated patent.[29] The microfabrication process, based on semiconductor manufacturing techniques, produced elements 150 μm thick with 200-μm spacing and areas ranging from 10 × 10 mm^2 and 4.9 × 4.9 mm^2 down to 2.35 × 2.35 mm^2. In total, each 3-in. (76.2 mm)-diameter wafer contained a total of 50 sensors (Figure S4; Note S2). Each sensor was designed with a varying number of turns, track widths, and spacing to ensure a unique electrical resonant frequency f_0. The average measured resonant frequencies of the sensors, f_{exp}, are within 6.9% ± 5.2% of the calculated value f_0 (Note S4).

As shown in Figure 2A, the resonant frequency f_0 of the sensors remains relatively constant and unaffected over 50 cycles of bending around a 1-mm radius plastic rod with no observable signs of damage to the tracks. This resilience is attributed to the wrinkled texture of the thin film metal tracks, as shown in Figure 2B, which provides effective mechanical relief of large compressive and tensile stresses due to the increased specific surface area.[30,31] This property of the sensor fabrication enables the sensors to be bent 180° without failure. Further testing demonstrates that the resonant frequencies of the sensors remain unchanged for up to five 180° folds before shifting to higher values, with the sensors remaining operational for up to 42 folds (Figure 2C). Crack generation is observed following repetitive folding but does not extend beyond a few micrometers near the initial site of the fracture and is limited only to the bending orientation, as shown in Figure 2D. In this case, the cracking can be primarily attributed to the overstrain and fracture of the track at the folding axis since the observed gap on the track is as large as 5 μm, with a clear axial dislocation of the two segments. At the same time, the metal wrinkles are believed to impede crack propagation, unlike the cracks generated on conventional planar metallization on PDMS. The film near the fracture has clearly undergone plastic deformation.[31,32]

Using the experimental setup shown in Figure 3A, the sensors successfully exhibit a pressure-dependent resonant frequency linear response that agrees with the theoretical model. Two regions are observed (shown in Figure 3B): a linear decrease of the resonant frequency, −1 MHz/100 Pa sensitivity for R^2 = 0.956 ± 0.430 at $P_c \leq 0.5$ kPa, and a gentler decrease, −0.6 MHz/1 kPa for R^2 = 0.989 ± 0.110 at $P_c > 0.5$ kPa. The ultra-low-pressure response can be attributed to the reduced effective Young's modulus of the frustra material/air gap system.[33] In both regimes, a higher sensitivity is recorded as the fundamental resonant frequency f_0 (p = 0 Pa) is increased. This is shown in Figure 3C for $P_c \leq 0.5$ kPa (R^2 = 0.707) and in Figure 3D for $P_c > 0.5$ kPa (R^2 = 0.767).

In vitro capsule testing

The five sensors, including sensors 1–4 on the body of the capsule to measure the contractile pressure and sensor 5 to measure the intraluminal pressure, are shown in Figures 4 and S10 (Note S5). The sensors were glued on a tethered capsule containing the integrated electronic subsystems (the three printed circuit boards [PCBs] named 2 to 4, containing the antenna and the PCB1). Pressure response was checked under simulated physiological conditions using a pneumatic intestinal phantom described in Note S5. Synchronous square waves at the clinically relevant frequencies of 0.15 and 0.25 Hz were used to induce a peristaltic contraction magnitude of 10 kPa (Figure 5A), as well as for higher pressures of ∼20 and 30 kPa (lower

Figure 2. Performance of the flexible LC sensors to repetitive bending and 180° folding

(A) Impact of repetitive bending over 1-mm radius on sensor resonant frequency.

(B) Left to right: increasing-magnification images of inductor tracks following 1-mm bending.

(C) Impact of repetitive 180° folding on sensor resonant frequency (the sensors were folded over the sharp width of a surgical blade, 250 μm thickness).

(D) Left to right: increasing-magnification images of inductor tracks following repetitive folding at 180°.

Please cite this article in press as: Mitrakos et al., PressureCap: An endoscopic sensor capsule for real-time gastrointestinal pressure monitoring, Device (2024), https://doi.org/10.1016/j.device.2024.100325

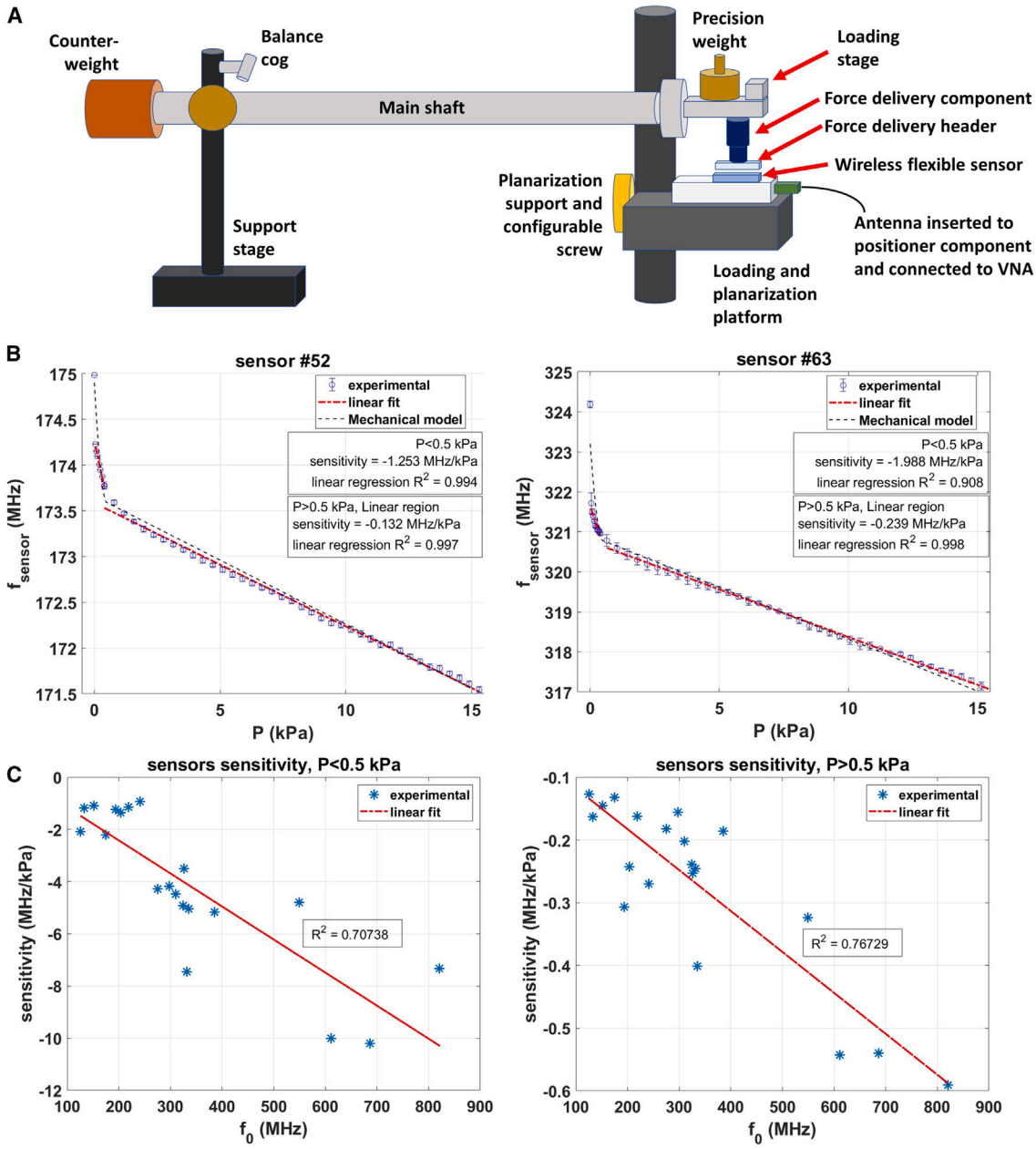

Figure 3. Performance of the LC sensors to dynamic characterization in the range of 0–15 kPa and against the theoretical model

(A) Schematic of experimental setup used to apply force to flexible sensors during characterization.

(B) Typical sensor response observed showing pressure dependency of sensor response and presence of 2 linear regions, an ultralow-pressure response for $P_c \leq 0.5$ kPa, and the other response at $P_c > 0.5$ kPa.

(C) Sensor sensitivity as a function of resonant frequency in the low-pressure (<0.5 kPa) region.

(D) Sensor sensitivity as a function of resonant frequency in the higher-pressure (>0.5 kPa) region.

Figures 5B and 5C). Similarly, slower arbitrary asynchronous waves, as expected in the GI tract, were generated at a variable magnitude of 0–30 kPa as shown in lower Figure 5D. The repeated application of compressive forces generated by the inflating phantom showed no sensor drift as the sensors returned to their fundamental frequency when the phantom deflated, as shown in Figure 5. The 200-Pa increments experienced by the sensors were detected via the tether using the external electronic readout system used to generate the square waves (Figure 4).

Peristaltic frequencies above 0.5 Hz exceeded the 0.35-Hz sampling frequency of the electronics integrated in the PCB1

Please cite this article in press as: Mitrakos et al., PressureCap: An endoscopic sensor capsule for real-time gastrointestinal pressure monitoring, Device (2024), https://doi.org/10.1016/j.device.2024.100325

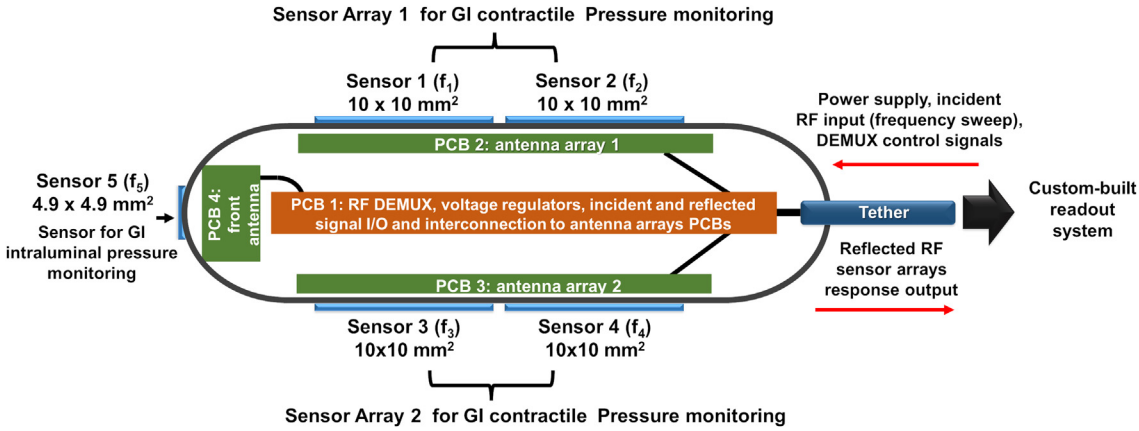

Figure 4. Schematic representation showing placement of various sensors, purpose of PCBs, and signal flow along tether to external readout system

of the capsule, resulting in undersampling of the pressure waves and a loss of fidelity, as shown in Figure S7. The sensors mounted on the sides of the shell demonstrate a linear response and good sensitivity, as shown in Figure 6, with −537 kHz/kPa for sensor 1 (R^2 = 0.998), −480 kHz/kPa for sensor 2 (R^2 = 0.976), −480.1 kHz/kPa for sensor 3 (R^2 = 0.967), and −479.9 kHz/kPa for sensor 4 (R^2 = 0.985). Mounting the sensors on the capsule shell imposed a precompression that drove the response of the sensors to the Pc > 0.5 kPa regime, as shown in Figure 6. Contact between the inflated inner surface of the phantom and the capsule was measured to be between 3 and 4 kPa for this capsule, given the size of the capsule (12 mm in diameter), and the occlusion rate of the 20-mm-diameter robotic actuator was at ∼40% occlusion at those pressure levels (the capsule was placed centrally in the robotic actuator).

In vivo capsule testing in porcine animal models

The tethered capsule was tested *in vivo* using a porcine model, as shown in Figure 7A. The measured pressure fluctuations in the GI tract were above the noise level and exceeded ΔP = ±0.4 kPa during all of the stages of the study. The front-mounted sensor—sensor 5 in Figure 4—recorded sinusoidal pressure fluctuations exceeding ±0.6 kPa at a constant frequency of 0.25 Hz, as shown in Figure 7B. The frequency of this signal suggests that it was generated by the mechanical ventilation apparatus controlling the respiration of the anesthetized pig. This was verified by a change in the acquired pressure signal, when mechanical ventilation was stopped temporarily to allow the animal to breathe unaided. The four sensors, sensors 1 to 4 in Figure 4, mounted on the cylindrical body of the shell captured a more complex signal than the sinusoidal signal detected by the front sensor. As shown in Figure 7C, the average amplitude of the complex pressure signal fluctuations was ΔP = ±0.5 kPa. These results are comparable to the signals detected by previously reported IMCs.[14] These complex pressure waves have been shown to be caused by a combination of the 1.17-Hz heartbeat, the respiration waves, the 0.3 kPa–0.43 kPa low-amplitude GI tract contractions (0.05–0.2 Hz[14,16]), and the baseline noise floor fluctuations of the sensor.[15]

Further evidence of the successful detection of GI motility was observed when prokinetics were administered. Asynchronous peristaltic GI motility was induced within ∼5 min of injection. This was observed using fluoroscopy. Video recorded by the fluoroscopic system showed capsule movement when in contact with the GI tract that corresponded to a change in body sensor signal (Video S1). Peristaltic pressure signals with amplitudes of up to 4 kPa were recorded by the sensors on the cylindrical part of the shell of the capsule in contact with the GI tract (Figure 7E), as well as with the front-mounted sensor (Figure 7F). The antisymmetric nature of the signals recorded by adjacent sensors on the capsule body shown in Figures 7G and 7H can be explained by the successive waves of compression and decompression induced by the peristaltic waves traveling the intestines.

DISCUSSION

The successful demonstration of the multisite pressure profile capability that the proposed IMC motility sensing approach provides is evidenced by the fact that the *in vivo* response of the sensors on the capsule surface is in good agreement regarding frequency of occurrence and magnitude levels with peristalsis. Future work will focus on the decomposition of this complex signal into its constituent physiological responses. The proof-of-concept capsule device was limited by a 0.2-kPa pressure resolution and a sampling frequency per sensor of 0.35 Hz, indicative of the upper sampling frequency limit of the electronics integrated in the PCB1 of capsule. This resulted in an undersampling of the fast physiological constituents such as the 1.17-Hz heartbeat. These limitations will be addressed in future work by redesigning the capsule system to enable simultaneous monitoring of all of the sensors at a higher sampling rate (>4 Hz) and with better resolution (<0.02 kPa). Further areas of improvement also include the need to miniaturize the sensor-reading electronics to fit within the capsule, ensuring an untethered capsule and enabling the integration of other clinically required

Please cite this article in press as: Mitrakos et al., PressureCap: An endoscopic sensor capsule for real-time gastrointestinal pressure monitoring, Device (2024), https://doi.org/10.1016/j.device.2024.100325

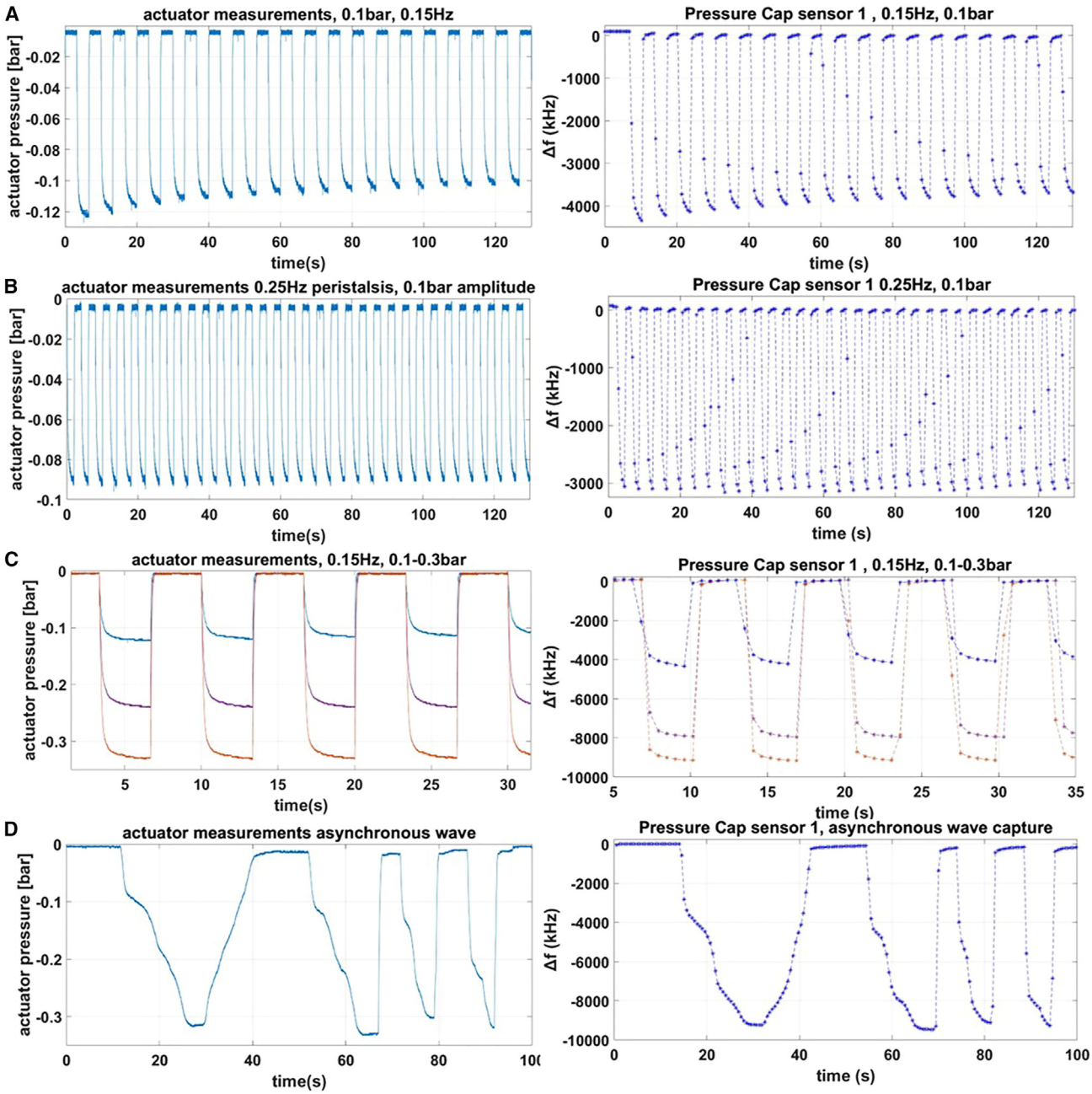

Figure 5. Peristaltic signals generated using pneumatic intestinal phantom (left) versus response measured using capsule
(right) for (A)–(D)
(A) 0.15 Hz, 10 kPa square waves.
(B) 0.25 Hz, 20 kPa square waves.
(C) 0.15 Hz signals of varying pressure.
(D) Asynchronous pressure waves.

systems such as optical imaging and wireless telemetry. One way that this can be achieved is through the design, fabrication, and integration of an application-specific integrated circuit that can replicate the capability of the current multichip PCBs onto a single integrated circuit.

EXPERIMENTAL PROCEDURES

Resource availability

Lead contact

Further information and requests for resources should be directed to and will be fulfilled by the lead contact, Marc Desmulliez (m.desmulliez@hw.ac.uk).

Please cite this article in press as: Mitrakos et al., PressureCap: An endoscopic sensor capsule for real-time gastrointestinal pressure monitoring, Device (2024), https://doi.org/10.1016/j.device.2024.100325

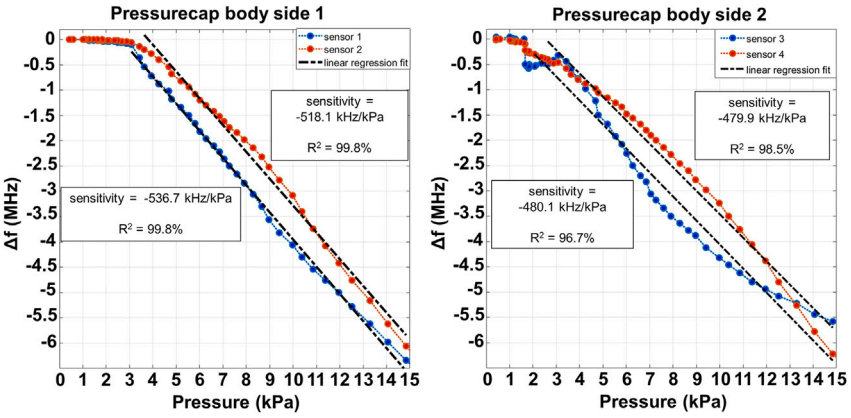

Figure 6. Characteristic response of the integrated sensors to pressure

Materials availability

This study did not generate new unique reagents.

Data and code availability

All of the raw data and original code associated with this work were deposited in Mendeley at https://doi.org/10.17632/5cbv57fckp.1.

Sensor characterization

The sensor response was characterized using an external planar antenna at a fixed 2.5-mm distance to the sensors and the Vector Network Analyser system (N5225A, Keysight, Santa Clara, CA). Dynamic characterization of the sensors was performed using a custom-built cantilever system, shown in Figure 3A, that applied a known compressive force to the sensors by varying the counterweight. This setup was used to measure the response of the sensors to pressures ranging from 0 to 10 kPa for the 10 × 10-mm^2 sensors and 0 to 15 kPa for the 4.9 × 4.9-mm^2 sensors. Static measurements for the 2.35 × 2.35-mm^2 sensors could not be undertaken using the external planar antenna at the fixed 2.5-mm distance because the separation distance was too large to obtain a measurable amplitude drop. The antenna was therefore placed directly above the sensor during static measurements of these sensors to obtain a measurable amplitude drop. This type of sensor was therefore deemed impractical for use and was not pursued further for dynamic characterization.

Capsule fabrication and assembly

The tethered capsule package, shown in Figure 8, consists of two additively manufactured components that, when connected together, form a 12-mm-diameter, 30-mm-long shell comparable to commercially available capsule endoscopes.[8] These half-shells were three-dimensionally (3D) printed using an Objet Connex 500 (Stratasys, Eden Prairie, MN) 3D printer equipped with Verowhite material. An array of 10 × 10-mm^2 sensors were fixed to the cylindrical body of each half-shell (body sensors 1–4) using a medical-grade instant adhesive (Loctite 4161, Henkel Adhesives, Dusseldorf, Germany). These sensors enable the assembled capsule to measure the contractile pressure. A single 4.9 × 4.9-mm^2 sensor (sensor 5) was similarly fixed to the front of the capsule to measure the luminal pressure. A 3-m-long silicone tether (TSR0400100P, Thermo Fisher Scientific, Waltham, MA) was attached to the other end of the capsule to enable physical communication between internal and external electronics and provide power to the internal electronic circuitry of the capsule. The assembled half-shells and the tether were fixed using a UV-curable biocompatible epoxy (Permabond 4UV80HV, Permabond, Pottstown, PA) according to the supplier's instructions.

The sensor response is acquired wirelessly via inductive coupling to an array of identical planar square multicoil antennas (4.5 × 4.5 mm^2 outer dimension, 150 μm track width, 175 μm track spacing, and 5.5 loops) located within the capsule. The antennas interrogating the body sensors 1–4 were printed on two PCBs (Eurocircuits, Mechelen, Belgium) fixed in place 2.5 mm underneath the upper and lower shells using slotted structures to ensure alignment with the sensors situated on the cylindrical surfaces (Figures 8B and S10; Note S5). Similarly, a 1-mm-thick, 7.2-mm-diameter circular PCB, PCB4, containing a single antenna is positioned 1.5 mm from the front sensor 5. Each sensor is sequentially addressed by a custom RF Demultiplexer (DEMUX) PCB, PCB1, located at the center of the capsule. All of the internal PCBs were connected together using 50-Ω microcoaxial JSC cables (MXJA01JA0200, Murata, Kyoto, Japan). Further details on the technical specifications of the PCBs are discussed in Note S3. Connections to external electronics and the RF MUX PCB are achieved using the tether cabling assembly located within the silicone tether tubing, which consists of five wires for DEMUX control and a shielded 26 AWG, 50-Ω coaxial cable (83259 009100, Belden, St. Louis, MO). Once assembled, the entire capsule was coated with an 8-μm-thick film of Parylene C using a vacuum deposition tool (SCS PDS 2010, Specialty Coating Systems, Indianapolis, IN). The surfaces were primed with A174 silane adhesion promoter before deposition. Parylene C is a US Pharmacopeia Class VI polymer that ensures biocompatibility, a good moisture barrier, and excellent lubricity. The mass of the assembled capsule is ~30 g.

Many of the electronics required to operate the device are located externally due to the limits of integration achievable with commercial off-the-shelf components for this proof-of-concept demonstrator. Previous studies by the authors also highlighted the upper limit of integration dictated by thermal output.[34] The external electronics, consisting of a custom-built, portable broadband reflectometer system, excite the antennas within the capsule with a sinusoidal signal sweeping in frequency from 1 MHz to 1 GHz in increments ≥10 kHz, depending on user need. The return loss amplitude, $|\Gamma|$, is measured for each frequency and used to determine the pressure-induced shift in the resonant frequency of each sensor. The system diagram in Figure 4 shows the connections between the external electronics and the capsule. Further details on the design and operation of the broadband reflectometer system can be found in Note S3.

In vitro capsule testing

In vitro characterization of the developed capsule device was carried out using a flexible silicone soft robotic actuator extensively described elsewhere.[35,36] This biomimetic system was previously used to emulate esophageal activity.[36] It consists of two components: a custom-built pump test bench and a silicone-based robotic actuator that generates controllable square-wave peristaltic motion at variable frequencies and pressures. Further details on the design and operation of the silicone-based robotic actuator system can be found in Note S5.

In vivo capsule testing

Porcine models were used to examine the performance of the developed capsule device due to the physiological and histological similarities of their GI tract with the human GI tract.[37] The experiment was conducted under the UK Home Office Licence (Procedure Project Licence 70/8812) in accordance with the UK Animal (Scientific Procedures) Act 1986. Two Landrace pigs (one male, one female), obtained from a local breeder, weighing in the range of 56–64 kg and aged 3–4 months, were used in this *in vivo* study. It was conducted at Dryden Farm, where the animals were kept in licensed housing (UK Project Establishment Licence 60/4604), bedded on straw, and fed rearer pellets (ABN, Cupar, UK). Before the study, food was withheld for 12 h but access to water was maintained until the preanesthetic medication was administered. General anesthesia was induced with intravenous propofol and maintained for the duration of the study with isoflurane (IsoFlo, Zoetis, Surrey, UK) vaporized in oxygen and nitrous oxide and delivered via a Bain breathing system. A cannula was placed in the auricular vein, and the trachea was intubated with Ringer's lactate solution (Aquapharm No. 11, Animalcare, York, UK)

Please cite this article in press as: Mitrakos et al., PressureCap: An endoscopic sensor capsule for real-time gastrointestinal pressure monitoring, Device (2024), https://doi.org/10.1016/j.device.2024.100325

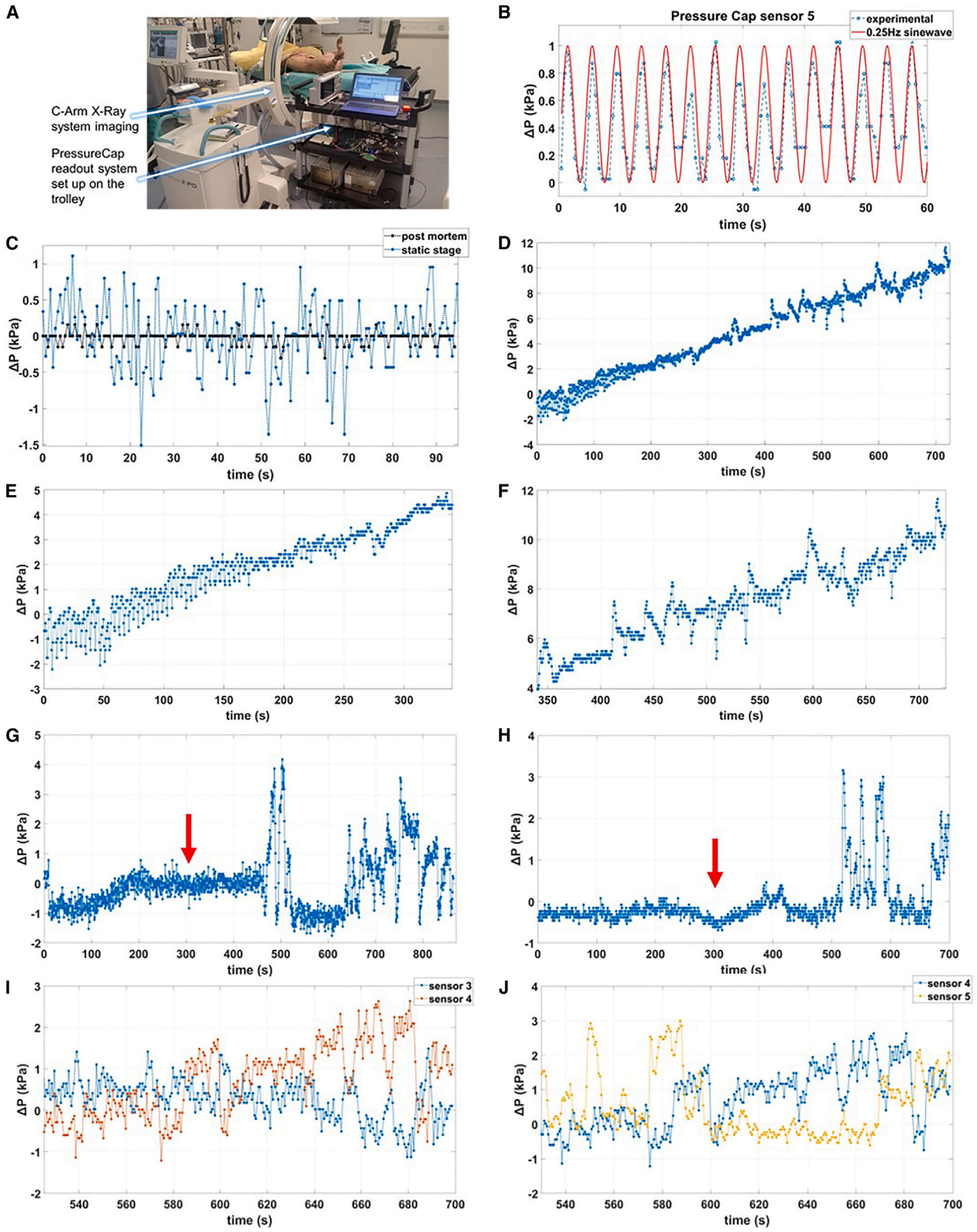

(legend on next page)

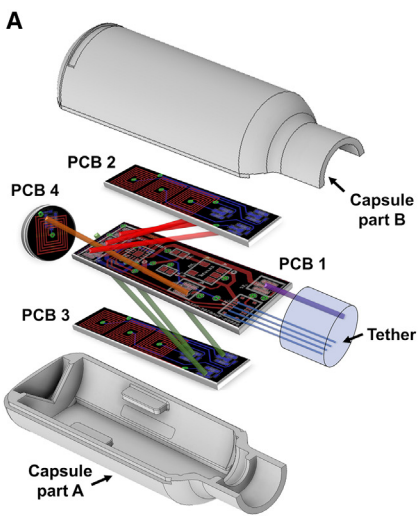

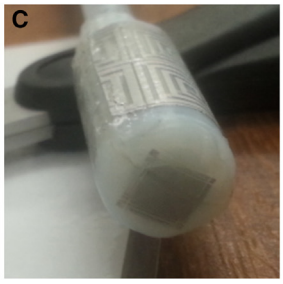

Figure 8. Depiction of the internal structure and integration of the capsule device

(A) Schematic representation showing placement of various sensors and thelocation of PCBs.

(B) Magnified view of the assembled capsule.

(C) Side image of assembled capsule showing contractile pressure sensors mounted on the device.

administered at 10 mL/kg/h throughout the trial to maintain fluid and electrolyte levels. The lungs of the anesthetized pigs were mechanically ventilated at 0.25 Hz to maintain normocapnia, and the vital signs of the animals were continuously monitored throughout the experiment by an experienced veterinary anesthetist. The animals were placed in a supine position, as shown in Figure 7A, and draped to maintain a normal body temperature. Access to the remote small intestine was gained by surgically creating a stoma immediately before the experiments. The capsule device was gently fed through the stoma until 30 cm of the tether, measured using a ruler, was inserted.

Following insertion of the capsule, 20 μg/kg neostigmine, a prokinetic, was administered to ensure GI motility because previous experiments with similar capsules found that GI motility was adversely affected by sedation and the creation of the stoma.[34,38] The effects of the prokinetic drug persist for a limited span of 5–10 min, forcing strong arbitrary aperiodic peristaltic contractions, and did not always induce motility as observed from previous porcine studies conducted by our group (unpublished data). Two doses of prokinetics were administered to each pig during each experiment, with at least 30 min between each dose.

Fluoroscopic imaging of the small intestine was initiated following administration of the prokinetic using a Ziehm Visio mobile C-arm X-ray system (Ziehm Imaging, Nuremberg, Germany) in conjunction with Gastrografin, a contrast agent for radiological examination. Imaging confirmed the effect of the prokinetics on GI motility and its effect on the capsule, as shown in Video S1. The equipment was used 4 times and 60 s during the prokinetics stage to ensure limited X-ray exposure to the clinical personnel. Following the experiments, the animals were euthanized using pentobarbital, with the capsule still residing within the small intestine. The capsule was collected postmortem.

SUPPLEMENTAL INFORMATION

Supplemental information can be found online at https://doi.org/10.1016/j.device.2024.100325.

ACKNOWLEDGMENTS

This work was supported by the UK Engineering and Physical Sciences Research Council (EPSRC) "Sonopill" Program Grant (EP/K034537/1, EP/K034537/2).

AUTHOR CONTRIBUTIONS

V.M. conceived the design; developed and characterized the microfabrication process of the sensors; designed, developed, and characterized the pressure capsule device and electronic readout system; designed and analyzed the theoretical model of the pressure sensor, the experimental design, and the data collection; and characterized and analyzed the sensors and pressure capsule device *in vitro* and *in vivo* performance. G.C. contributed to the design of the *in vivo* trial, assembly of the capsule, and writing of the manuscript. F.J.T. contributed to the *in vitro* testing of the capsule. B.F.C. contributed to the design and execution of the *in vivo* trial. S.K.P. contributed to the testing of the sensors. G.S.W. contributed to sensor fabrication. M.A.P. contributed to the design of the *in vivo* trial and reviewed the manuscript. E.C. contributed to all aspects of the *in vivo* trial and reviewed the manuscript. S.C. led the preparation of the project funding proposal, contributed to the experimental design, and reviewed the manuscript. T.S. contributed to the *in vitro* trial with the tissue phantom and reviewed the manuscript. P.J.W.H. contributed

Figure 7. Porcine *in vivo* experiment of the capsule device and detection of peristaltic events

(A) Experimental setup for *in vivo* tests with porcine animal model.

(B) Response from front-mounted sensor capturing mechanical ventilation of porcine subject.

(C) Capture of low-amplitude peristaltic activity from body-mounted sensors superimposed with postmortem measurements (black line).

(D) Impact of temporary deactivation of mechanical ventilation of porcine subject on front-mounted sensor response from 200 s onward.

(E) Magnified view of pressure response of front-mounted sensor during active mechanical ventilation.

(F) Magnified view of pressure response of front-mounted sensor during deactivated mechanical ventilation.

(G) Change in measured contractile pressure upon administration of prokinetics from side-mounted sensor (arrow signifies approximate administration of prokinetics).

(H) Change in measured intraluminal pressure upon administration of prokinetics from front-mounted sensor (arrow signifies approximate administration of prokinetics).

(I and J) Closeup comparison between different sensors of the capsule of the captured peristaltic waves during the prokinetics experiment: (I) sensors 3 and 4 and (J) sensors 4 and 5.

to sensor design, fabrication, and testing and reviewed the manuscript. M.P.Y.D. contributed to the conception and design of the sensors microfabrication process and the pressure capsule, conceived and designed the theoretical model of the pressure sensor, and reviewed the manuscript.

DECLARATION OF INTERESTS

The authors declare no competing interests.

Received: October 3, 2023
Revised: October 6, 2023
Accepted: February 23, 2024
Published: March 19, 2024

REFERENCES

1. Anderson, P., Dalziel, K., Davies, E., Fitzsimmons, D., Hale, J., Hughes, A., Isaac, J., Onishchenko, K., Phillips, C., and Pockett, R. (2014). Survey of digestive health across Europe: Final report. Part 2: The economic impact and burden of digestive disorders. United European Gastroenterol. J. *2*, 544–546. https://doi.org/10.1177/2050640614554155.
2. Fox, M.R., Kahrilas, P.J., Roman, S., Gyawali, C.P., Scott, S.M., Rao, S.S., Keller, J., and Camilleri, M. (2018). Clinical measurement of gastrointestinal motility and function: who, when and which test? Nature reviews Gastroenterology & hepatology *15*, 568–579. https://doi.org/10.1038/s41575-018-0030-9 10.
3. Talley, N.J. (2008). Functional gastrointestinal disorders as a public health problem. Neuro Gastroenterol. Motil. *20*, 121–129. https://doi.org/10.1111/j.1365-2982.2008.01097.x.
4. Halder, S.L.S., Locke, G.R., Schleck, C.D., Zinsmeister, A.R., Melton, L.J., and Talley, N.J. (2007). Natural History of Functional Gastrointestinal Disorders: A 12-year Longitudinal Population-Based Study. Gastroenterology *133*, 799–807. https://doi.org/10.1053/j.gastro.2007.06.010.
5. Saad, R.J., and Hasler, W.L. (2011). A technical review and clinical assessment of the wireless motility capsule. Gastroenterol. Hepatol. *7*, 795–804.
6. Wang, W.X., Yan, G.Z., Sun, F., Jiang, P.P., Zhang, W.Q., and Zhang, G.F. (2005). A non-invasive method for gastrointestinal parameter monitoring. World J. Gastroenterol. *11*, 521–524. https://doi.org/10.3748/wjg.v11.i4.521.
7. Cummins, G. (2021). Smart pills for gastrointestinal diagnostics and therapy. Adv. Drug Deliv. Rev. *177*, 113931. https://doi.org/10.1016/j.addr.2021.113931.
8. Cummins, G., Cox, B.F., Ciuti, G., Anbarasan, T., Desmulliez, M.P.Y., Cochran, S., Steele, R., Plevris, J.N., and Koulaouzidis, A. (2019). Gastrointestinal diagnosis using non-white light imaging capsule endoscopy. Nat. Rev. Gastroenterol. Hepatol. *16*, 429–447. https://doi.org/10.1038/s41575-019-0140-z.
9. Stein, E., Berger, Z., Hutfless, S., Shah, L., Wilson, L.M., Haberl, E.B., Bass, E.B., and Clarke, J.O. (2013). Wireless Motility Capsule versus Other Diagnostic Technologies for Evaluating Gastroparesis and Constipation: A Comparative Effectiveness Review (Agency for Healthcare Research and Quality (US)).
10. Kuo, B., Maneerattanaporn, M., Lee, A.A., Baker, J.R., Wiener, S.M., Chey, W.D., Wilding, G.E., and Hasler, W.L. (2011). Generalized Transit Delay on Wireless Motility Capsule Testing in Patients with Clinical Suspicion of Gastroparesis, Small Intestinal Dysmotility, or Slow Transit Constipation. Dig. Dis. Sci. *56*, 2928–2938. https://doi.org/10.1007/s10620-011-1751-6.
11. FDA Food and Drink Administration. Smartpill GI Monitoring System. Market approval notification version 2.0. https://www.accessdata.fda.gov/scripts/cdrh/cfdocs/cfpmn/pmn.cfm?ID=K092342.
12. Tran, K., Brun, R., and Kuo, B. (2012). Evaluation of regional and whole gut motility using the wireless motility capsule: relevance in clinical practice. Therap. Adv. Gastroenterol. *5*, 249–260. https://doi.org/10.1177/1756283X12437874.
13. Arshak, A., Arshak, K., Waldron, D., Morris, D., Korostynska, O., Jafer, E., and Lyons, G. (2005). Review of the potential of a wireless MEMS and TFT microsystems for the measurement of pressure in the GI tract. Med. Eng. Phys. *27*, 347–356. https://doi.org/10.1016/j.medengphy.2004.11.002.
14. Li, P., Kreikemeier-Bower, C., Xie, W., Kothari, V., and Terry, B.S. (2017). Design of a Wireless Medical Capsule for Measuring the Contact Pressure Between a Capsule and the Small Intestine. J. Biomech. Eng. *139*, 051003. https://doi.org/10.1115/1.4036260.
15. Woo, S.H.A., Mohy-Ud-Din, Z., and Cho, J.H. (2013). Telemetry capsule for measuring contractile motion in the small intestine. Biomed. Microdevices *15*, 63–72. https://doi.org/10.1007/s10544-012-9688-x.
16. Li, P., Kothari, V., and Terry, B.S. (2015). Design and Preliminary Experimental Investigation of a Capsule for Measuring the Small Intestine Contraction Pressure. IEEE Trans. Biomed. Eng. *62*, 2702–2708. https://doi.org/10.1109/TBME.2015.2444406.
17. Kloetzer, L., Chey, W.D., Mccallum, R.W., Koch, K.L., Wo, J.M., Sitrin, M., Katz, L.A., Lackner, J.M., Parkman, H.P., Wilding, G.E., et al. (2010). Motility of the antroduodenum in healthy and gastroparetics characterized by wireless motility capsule. Neuro Gastroenterol. Motil. *22*, 527–e117. https://doi.org/10.1111/j.1365-2982.2010.01468.x.
18. Hasler, W.L., Saad, R.J., Rao, S.S., Wilding, G.E., Parkman, H.P., Koch, K.L., McCallum, R.W., Kuo, B., Sarosiek, I., Sitrin, M.D., et al. (2009). Heightened colon motor activity measured by a wireless capsule in patients with constipation: relation to colon transit and IBS. Am. J. Physiol. Gastrointest. Liver Physiol. *297*, G1107–G1114. https://doi.org/10.1152/ajpgi.00136.2009.
19. Ruth, S.R.A., Feig, V.R., Tran, H., and Bao, Z. (2020). Microengineering Pressure Sensor Active Layers for Improved Performance. Adv. Funct. Mater. *30*, 2003491. https://doi.org/10.1002/adfm.202003491.
20. Mitrakos, V., Hands, P.J.W., Cummins, G., Macintyre, L., Denison, F.C., Flynn, D., and Desmulliez, M.P.Y. (2018). Nanocomposite-Based Microstructured Piezoresistive Pressure Sensors for Low-Pressure Measurement Range. Micromachines *9*, 43. https://doi.org/10.3390/mi9020043.
21. Nabar, B.P., Celik-Butler, Z., and Butler, D.P. (2015). Self-Powered Tactile Pressure Sensors Using Ordered Crystalline ZnO Nanorods on Flexible Substrates Toward Robotic Skin and Garments. IEEE Sensor. J. *15*, 63–70. https://doi.org/10.1109/JSEN.2014.2337115.
22. Zhu, G., Yang, W.Q., Zhang, T., Jing, Q., Chen, J., Zhou, Y.S., Bai, P., and Wang, Z.L. (2014). Self-Powered, Ultrasensitive, Flexible Tactile Sensors Based on Contact Electrification. Nano Lett. *14*, 3208–3213. https://doi.org/10.1021/nl5005652.
23. Boutry, C.M., Nguyen, A., Lawal, Q.O., Chortos, A., Rondeau-Gagné, S., and Bao, Z. (2015). A Sensitive and Biodegradable Pressure Sensor Array for Cardiovascular Monitoring. Adv. Mater. *27*, 6954–6961. https://doi.org/10.1002/adma.201502535.
24. Chen, P.-J., Saati, S., Varma, R., Humayun, M.S., and Tai, Y.-C. (2010). Wireless Intraocular Pressure Sensing Using Microfabricated Minimally Invasive Flexible-Coiled LC Sensor Implant. J. Microelectromech. Syst. *19*, 721–734. https://doi.org/10.1109/JMEMS.2010.2049825.
25. Chitnis, G., Maleki, T., Samuels, B., Cantor, L.B., and Ziaie, B. (2013). A Minimally Invasive Implantable Wireless Pressure Sensor for Continuous IOP Monitoring. IEEE Trans. Biomed. Eng. *60*, 250–256. https://doi.org/10.1109/TBME.2012.2205248.
26. Luo, M., Martinez, A.W., Song, C., Herrault, F., and Allen, M.G. (2014). A Microfabricated Wireless RF Pressure Sensor Made Completely of Biodegradable Materials. J. Microelectromech. Syst. *23*, 4–13. https://doi.org/10.1109/JMEMS.2013.2290111.
27. Chen, L.Y., Tee, B.C.-K., Chortos, A.L., Schwartz, G., Tse, V., Lipomi, D.J., Wong, H.-S.P., McConnell, M.V., and Bao, Z. (2014). Continuous wireless pressure monitoring and mapping with ultra-small passive sensors for

health monitoring and critical care. Nat. Commun. *5*, 5028. https://doi.org/10.1038/ncomms6028.

28. Boutry, C.M., Beker, L., Kaizawa, Y., Vassos, C., Tran, H., Hinckley, A.C., Pfattner, R., Niu, S., Li, J., Claverie, J., et al. (2019). Biodegradable and flexible arterial-pulse sensor for the wireless monitoring of blood flow. Nat. Biomed. Eng. *3*, 47–57. https://doi.org/10.1038/s41551-018-0336-5.
29. Hands P.J.W., Mitrakos V., MacIntyre L.M., Desmulliez M.P.Y. Flexible devices incorporating electronically-conductive layers, including flexible wireless LC sensors. Patent Number WO2021171037A1.
30. Rodríguez-Hernández, J. (2015). Wrinkled interfaces: Taking advantage of surface instabilities to pattern polymer surfaces. Prog. Polym. Sci. *42*, 1–41. https://doi.org/10.1016/j.progpolymsci.2014.07.008.
31. Yu, S., Zhang, X., Xiao, X., Zhou, H., and Chen, M. (2015). Wrinkled stripes localized by cracks in metal films deposited on soft substrates. Soft Matter *11*, 2203–2212. https://doi.org/10.1039/C5SM00105F.
32. Polywka, A., Stegers, L., Krauledat, O., Riedl, T., Jakob, T., and Görrn, P. (2016). Controlled Mechanical Cracking of Metal Films Deposited on Polydimethylsiloxane (PDMS). Nanomaterials *6*, 168. https://doi.org/10.3390/nano6090168.
33. Tee, B.C.-K., Chortos, A., Dunn, R.R., Schwartz, G., Eason, E., and Bao, Z. (2014). Tunable Flexible Pressure Sensors using Microstructured Elastomer Geometries for Intuitive Electronics. Adv. Funct. Mater. *24*, 5427–5434. https://doi.org/10.1002/adfm.201400712.
34. Lay, H.S., Cummins, G., Cox, B.F., Qiu, Y., Turcanu, M.V., McPhillips, R., Connor, C., Gregson, R., Clutton, E., Desmulliez, M.P.Y., and Cochran, S. (2019). In-Vivo Evaluation of Microultrasound and Thermometric Capsule Endoscopes. IEEE Trans. Biomed. Eng. *66*, 632–639. https://doi.org/10.1109/TBME.2018.2852715.
35. Esser, F., Krüger, F., Masselter, T., and Speck, T. (2018). Development and Characterization of a Novel Biomimetic Peristaltic Pumping System with Flexible Silicone-Based Soft Robotic Ring Actuators. In Biomimetic and Biohybrid Systems Lecture Notes in Computer Science, V. Vouloutsi, J. Halloy, A. Mura, M. Mangan, N. Lepora, T.J. Prescott, and P.F.M.J. Verschure, eds. (Springer International Publishing), pp. 157–167. https://doi.org/10.1007/978-3-319-95972-6_17.
36. Esser, F., Steger, T., Bach, D., Masselter, T., and Speck, T. (2017). Development of Novel Foam-Based Soft Robotic Ring Actuators for a Biomimetic Peristaltic Pumping System. In Biomimetic and Biohybrid Systems Lecture Notes in Computer Science, M. Mangan, M. Cutkosky, A. Mura, P.F.M.J. Verschure, T. Prescott, and N. Lepora, eds. (Springer International Publishing), pp. 138–147. https://doi.org/10.1007/978-3-319-63537-8_12.
37. Swindle, M.M., Makin, A., Herron, A.J., Clubb, F.J., and Frazier, K.S. (2012). Swine as Models in Biomedical Research and Toxicology Testing. Vet. Pathol. *49*, 344–356. https://doi.org/10.1177/0300985811402846.
38. Norton, J.C., Slawinski, P.R., Lay, H.S., Martin, J.W., Cox, B.F., Cummins, G., Desmulliez, M.P.Y., Clutton, R.E., Obstein, K.L., Cochran, S., and Valdastri, P. (2019). Intelligent magnetic manipulation for gastrointestinal ultrasound. Sci. Robot. *4*, eaav7725. https://doi.org/10.1126/scirobotics.aav7725.